Agostino Stilli, Helge A Wurdemann and Kaspar Althoefer, Shrinkable, stiffness-controllable soft manipulator based on a bio-inspired antagonistic actuation principle, in IEEE International Conference on Intelligent Robots and Systems, 2014, pp. 2476-2481. (DOI: 10.1109/IROS.2014.6942899)

Shrinkable, stiffness-controllable soft manipulator based on a bio-inspired antagonistic actuation principle

Agostino Stilli, Helge A Wurdemann and Kaspar Althoefer, *Member, IEEE*

***Abstract*— This paper explores a new hybrid actuation principle combining pneumatic and tendon-driven actuators for a soft robotic manipulator. The fusion of these two actuation principles leads to an overall antagonistic actuation mechanism whereby pneumatic actuation opposes tendon actuation - a mechanism commonly found in animals where muscles can oppose each other to vary joint stiffness. We are taking especially inspiration from the octopus who belongs to the class of Cephalopoda; the octopus uses its longitudinal and transversal muscles in its arms to achieve varied motion patterns; activating both sets of muscles, the octopus can control the arm stiffness over a wide range. Our approach mimics this behavior and achieves comparable motion patterns, including bending, elongation and stiffening. The proposed method combines the advantages of tendon-driven and pneumatic actuated systems and goes beyond what current soft, flexible robots can achieve: because the new robot structure is effectively an inflatable, sleeve, it can be pumped up to its fully inflated volume and, also, completely deflated and shrunk. Since, in the deflated state, it comprises just its outer "skin" and tendons, the robot can be compressed to a very small size, many times smaller when compared to its fully-inflated state. In this paper, we describe the mechanical structure of the soft manipulator. Proof-of-concept experiments focus on the robot's ability to bend, to morph from completely shrunk to entirely inflated as well as to vary its stiffness.**

I. INTRODUCTION

Over past decades, researchers have created a number of different robotic manipulator types that can be categorized into different classes, including discrete, serpentine and continuum robots [1]. Traditional robots inspired by human limbs are made of discrete rigid links that are connect by low degrees of freedom (DOF) joints. However, taking inspiration from animals such as the octopus, continuum robot tentacles have been created that have theoretically an infinite number of DOFs. The actual DOF depends to a large extend also on the actuation method employed. With respect to continuum robotic manipulators, the actuation mechanisms can be classified into intrinsic, extrinsic and hybrid actuation [1], [2].

The most common extrinsic actuation mechanisms are based on tendons to drive the joints of a manipulator. Thin tendons or cables are guided along the robot and fixed at the tip and intermediate points. Externally placed motors control the length of each cable as, for instance, realized in cardiac catheter robots described in [3]. The DOF depends on the number of integrated tendons and fix points along the manipulator [4]. Other examples of such manipulators using tendon-based actuation can be found in [5]–[11]. Tendon-driven manipulators can usually not extend their structure in longitudinal direction. Another recent approach to continuum manipulators is based on extrinsically actuated concentric tubes, with applications in the field of Minimally Invasive Surgery (MIS) [12]–[14]. Hollow, pre-curved and flexible cannulas are longitudinally moved inside each other and hence gradually extend the manipulator. Applying a rotational motion to one or multiple segments results in a variation of the robot's shape.

Taking inspiration from the octopus, a number of intrinsically actuated manipulators have been created: The Octarm manipulator is equipped with a set of in series connected actuators [15]. A universal joint based flexible robot for MIS was developed in [16]. The articulated sections are actuated by seven embedded micro-motors allowing the development of a miniaturized structure with a diameter of 12 mm. In the OCTOPUS project, a flexible octopus-like arm was fabricated from a series of shape memory alloy active spring actuators mimicking the contraction and elongation behavior of the biological role model [17]. Whereas the OCTOPUS robot was developed with the intention to be as close to nature as possible, the STIFF-FLOP project investigates how the features of an octopus can be exploited to create medical devices [18] with embedded sensors [19]–[21]. The current STIFF-FLOP robot prototype consists of a silicon body with three equally spaced hollow chambers embedded within and arranged in a radial fashion along

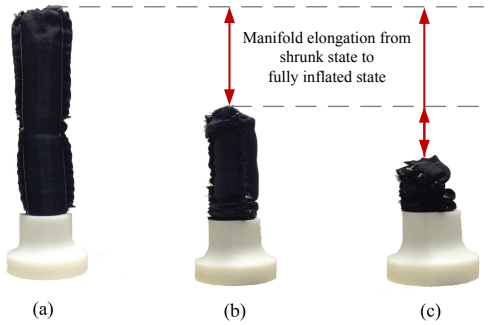

Fig. 1. Prototype of the shrinkable, stiffness-controllable manipulator in the (a) stiff and elongated state, (b) intermediate state, and (c) entirely shrunk state.

*The work described in this paper is partially funded by the Seventh Framework Programme of the European Commission under grant agreement 287728 in the framework of EU project STIFF-FLOP.

Agostino Stilli, Helge A Wurdemann and Kaspar Althoefer are with King's College London, Department of Informatics, Centre for Robotics Research, Strand, London, WC2R 2LS, United Kingdom agostino.stilli, helge.wurdemann, k.althoefer@kcl.ac.uk

the longitudinal axis; the chambers are pneumatically actuated [22]; Stiffness control is achieved using granular jamming inside an additional chamber within the silicone structure [23]. In [24], researchers proposed the use of polymeric artificial muscles to actuate a robot manipulator. This type of actuation mechanism was extended by incorporating granular jamming compartments capable of actuating, softening and stiffening the joints along the length of the manipulator [25].
Combining two types of actuation principles leads often to enhanced manipulation capabilities compared when only a single actuation principle is employed [2], including the improved control of the robot's configuration, stiffness and compliance. An example of a hybrid robot concept can be found in [26] where pneumatic artificial muscles are integrated with small electrical motors. In [27], extrinsically and intrinsically actuation mechanisms were fused. This concept of pneumatic and tendon-driven actuation was then further investigated in [28]; each module consists of a pressurizable non-stretchable hose inside an outer hose and a set of tendons that are connected to aluminum plates at the tip and bottom of each module.

In our paper, we propose the integration of an entirely soft outer sleeve with a hybrid actuation approach that employs pneumatic and tendon-driven actuation mechanisms, to realize a new type of robotic manipulator that can elongate along its longitudinal axis over a wide range, bend in all directions away from the longitudinal axis and change its stiffness. The proposed manipulator is entirely soft consisting of modules that are constructed of an internal stretchable, air-tight bladder integrated with an outer, non-stretchable polyester fabric sleeve that prevents ballooning. Tendons connected to the distal ends of the robot modules run along the outer sleeve allowing each module to bend. The created prototype is shown in Figure 1.
The content of this paper is organized as follows: Section II highlights the main contributions and novel features of the proposed hybrid actuation system. The mechanical design of the manipulator and the interface for motion control are described in Section III. To show the feasibility of the combination of tendon-based and pneumatic actuation, several experiments have been conducted (see Section IV). The results highlight the main advantages of the proposed technique when compared to traditional, intrinsically or extrinsically actuated robots.

II. CHARACTERIZATION OF THE BIOLOGICALLY-INSPIRED MECHANISM

A. Inspiration by Antagonistic Tissue Behavior in Octopus Arms

The proposed approach is inspired by biology - the role model for our research are the limbs of the octopus. Specifically, the proposed actuation approach is antagonistic in its nature as it is the case in the above animals as well as many other animal and humans. Two sets of muscles "collaborate" in an opposing way to actuate a link or a link segment, such as an arm. The octopus has longitudinal and transversal muscles in its arms and activating both sets of muscles, the octopus arms can be stiffened [29], [30] (see Figure 2). In octopus arms, biologists speak about the connecting tissue that keeps the muscles of the octopus arms in place, avoiding bulging and allowing the animal to achieve stiffness in their arms (comparable to a tube inside a bicycle tire). A similar behavior is achieved with the hybrid manipulation principle presented here.

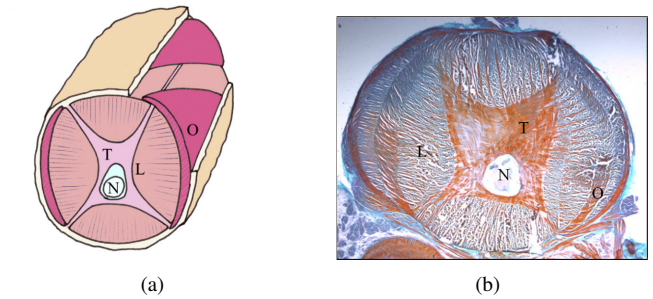

(a) (b)

Fig. 2. Anatomic muscle structure of an octopus arm [31]: (O) oblique, (T) transverse, and (L) longitudinal muscles; (N) nerve cord.

B. Characterization of the Soft Manipulator

The proposed hybrid actuation mechanism combines the advantages of tendon-driven (extrinsic) and pneumatic (intrinsic) actuation mechanisms. It has been shown that due to their thin structure and high tensile strength, tendons can be employed to operate large manipulators [15] as well as miniaturize robots [3]. Fairly accurate position control can be achieved using tendons. The motors used to control the length of the tendons or cables are most commonly placed outside the robot's main structure; hence, the maximum forces that can be applied depend on the tensile strength of the tendons and the maximum force that can be generated by the motors. On the other hand, the main advantage of pneumatic actuated robots is their capability to be compliant - and are, thus, particularly suited for us in the vicinity of humans. Combining these two actuation principles, the manipulation concept proposed in this paper has the following characteristics:

1) The robot is able to morph between the extreme states of being entirely shrunk and completely elongated. As the structure only consists of tendons, an internal latex bladder and an outer sleeve made of fabric, an extension of factor 20 or more is possible.
2) Inflating the robot (outward moving) and tightening the tendons at the same time, varying degrees of stiffness can be achieved.
3) Due to the robot's structure that makes do without a backbone or an external skeleton, the manipulator can be squeezed through narrow openings and is still fully functional.
4) The manipulator is fundamentally a simple structure which lends itself very well to miniaturization.

It is noted that in addition to the above considerations, for the design of the manipulator prototype described here, only materials have been used that do not affect the homogeneity of magnetic resonance (MR) images, hence, the proposed robot is MR-safe and lends itself to be used during MR-guided MIS.

III. DESIGN OF THE HYBRID ACTUATION MECHANISM

A. Structure and Assembly of the Manipulator

Exploded and assembled views of the manipulator are shown in Figures 3(a) and (b), respectively. The robot structure is composed of three main components: an inner air-tight and stretchable latex bladder, an outer, non-stretchable (but shrinkable) polyester fabric sleeve and three pairs of nylon tendons. The stretchable cylindrical latex bladder is inserted into the cylindrical polyester sleeve. The outer sleeve is 20 cm in length and has a diameter of 23 mm, when fully inflated. As the fabric material is non-stretchable, the outer sleeve prevents any ballooning of the inner bladder in radial direction beyond the maximum diameter of 23 mm. Whilst morphing from a deflated state to an inflated state, the robot can only expand along its longitudinal axis (elongation). The stiffness of the arm can be controlled by adjusting the tendons appropriately - e.g. tightening the tendons at a given air pressure in the sleeve will reduce the robot's length and increase the stiffness. In order to avoid the latex sleeve from being twisted inside the manipulator whilst extending, the tip of the latex bladder is attached to the tip of the outer sleeve. The nylon tendons are guided along the outside of the manipulator sleeve within polyester channels, 120° spaced apart along the perimeter of the outer sleeve. In our two-module prototype, three tendons are fixed to the tip of the manipulator and another set of three tendons are attached to the tip of the proximal module (i.e. the middle of the manipulator). Employing this approach, the robot's two modules can be independently controlled, Figures 3 and 4.

B. Active Motion Control Setup

Figure 4 gives a schematic overview of the setup of the whole system. The inner latex bladder is connected to one pressure regulator (SMC ITV0010-3BS-Q). The regulator is able to control the air pressure from 0.001 MPa to 0.1 MPa capable of inflating and deflating the inner bladder of the robot. An air compressor (BAMBI MD Range Model 150/500) ensures the supply with sufficient pressure limited to the maximum pressure the regulators can cope with.

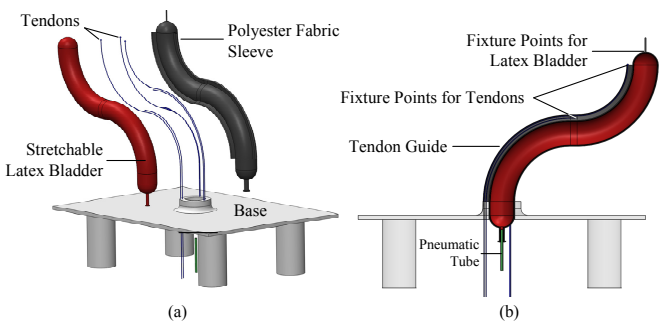

Fig. 3. CAD drawing of the structure for the novel soft manipulator: (a) Exploded view and (b) Assembled view.

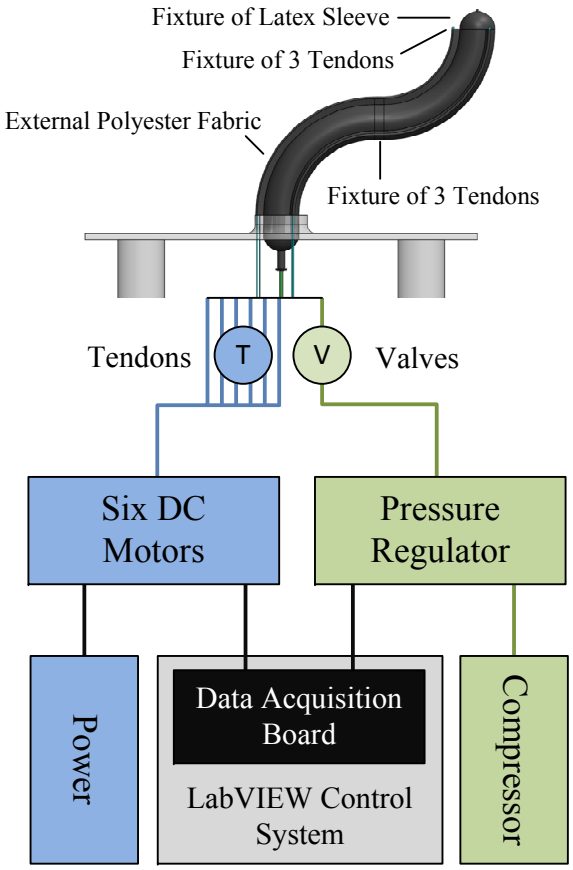

Fig. 4. Initial active motion control architecture involving DC motors (tendon actuation) and a pressure regulator (pneumatic actuation).

The tendons are connected via a pulley system of a 6.4 mm radius to six DC motors (Maxon RE-max 24). The gear (Maxon Planetary Gearhead GP 22 C) provides a maximum torque of 2 Nm which results in a maximum of 312.5 N considering the dimension of the pulleys.

The DC motors and pressure regulators are interfaced via a DAQ card (NI USB-6211) to LabVIEW software. A joystick (Logic 3 JS282 PC Joystick) is utilized to steer the hybrid actuation system: The toggle drives the tendon pulleys mounted to the DC motors controlling the angular position of the shaft and hence controls the bending of the manipulator. In combination with the tendon actuation, a button is configured to regulate the pressure inside the latex sleeve. Being able to steer the manipulator using the tendons and regulating the pressure at the same time, allows keeping constant pressure when the deflatable arm shrinks, extends or bends on the one hand and to control the stiffness (increasing the pressure in the latex bladder) when pulling all tendons simultaneously on the other hand. In this way, a motion control architecture was implemented in order to conduct the experiments in Section IV.

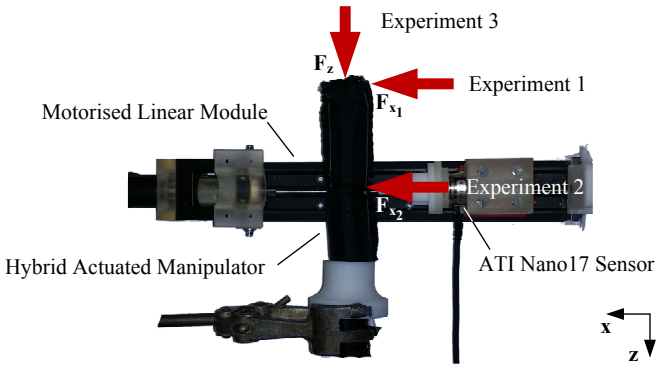

Fig. 5. Experimental setup for stiffness tests with a ATI Nano17 Force/Torque sensor using a motorized linear module.

IV. EXPERIMENTAL TESTS AND RESULTS

A. Experimental Setup

In order to explore the manipulator's ability to change stiffness, experiments were conducted applying lateral forces $\vec{F}_x$ and longitudinal forces $\vec{F}_z$ to the manipulator (see Figure 5). The experiments consisted of loading and unloading the robot up to a 15 mm deflection. The resulting load forces were measured by an ATI Nano17 Force/Torque sensor. The loading phases were controlled by a motorized linear module at a speed of $0.25\,\frac{\text{mm}}{\text{s}}$. The unloading phases are identical to the load phases, with the exception that the module is moving in the opposite direction to its initial position. The overall experimental setup is shown in Figure 5. Forces were applied at three different locations while the tendons were not actuated by the pulleys in order to evaluate the stiffness variation in a static condition. The results are reported in Section IV-B and IV-C respectively.
Data from the force sensor and the linear module were recorded at 1 kHz using a DAQ card (NI USB-6211). Four trials were performed for each deflection location, and with the average and variability of each point plotted against the deflection distance.

B. Lateral Forces (Experiment 1 and 2)

The results of Experiments 1 and 2 (Figure 5) measuring the load and unload forces are shown in Figures 6 to 8. The curves showing load forces (or forward motions) of the manipulator start in the origin of the coordinate frame $(0,0)$ for all figures. Figure 6 gives an example of the raw data recorded by the force/torque sensor when deflecting the manipulator tip by 15 mm over four trials. The pressure applied to the latex bladder was 0.015 MPa in this case.
In Experiment 1, a displacement of 15 mm was applied to the robot's tip. The lateral forces $\vec{F}_{x_1}$ were recorded and can be seen in Figure 7. In Figure 7(a), the manipulator's internal bladder had a constant pressure of 0.0075 MPa; a pressure of 0.015 MPa was recorded in Figure 7(b). From the graphs, the manipulator with lower pressure exhibited a fairly linear profile, reaching a peak of 0.9 N. When the pressure was increased to a higher value, the robot displayed a non-linear behavior during the displacements test, reaching a maximum force $\vec{F}_{x_1}$ of 1.4 N. The hysteresis and average variability were significantly lower when applying a higher pressure.
Figure 8 show the results of Experiment 2. Here, a lateral force $\vec{F}_{x_2}$ was recorded when deflecting the center of the manipulator. From Figure 7(a), the maximum force achieved is 4.8 N for a pressure of 0.0075 MPa. When raising the value to 0.015 MPa, a force of 9.5 N was measured. Similar to the results of Experiment 2, the hysteresis is lower for a stiffer manipulator.
From Experiments 1 and 2, it can be noted that the amount of lateral force increases and the hysteresis decreases with higher pressures applied to the latex bladder during deflections.

C. Longitudinal Forces (Experiment 3)

In Experiment 3, forces $\vec{F}_z$ were measured during longitudinal displacements of 15 mm at the manipulator tip. The results are reported in Figure 9. Figure 9(a) shows results for pressure values of 0.0075 MPa. During the experiments, a maximum force of 1.6 N was achieved. A force of 3.5 N was reached for a pressure of 0.015 MPa in Figure 9(b). Both experimental results show a non-linear profile. A similar effect as in Experiments 1 and 2 with regards to the hysteresis behavior can be noted here. However, the average variability is 0.3 N which is significantly larger than during Experiments 1 and 2. This is due to the non-linear ballooning effect of the internal latex bladder during the unloading sequence.

D. Bending Behavior

In order to show the working space and bending behavior, experiments have been conducted actuating the tendons that are fixed at the tip and middle section of the manipulator. The results were captured for robot movements in one plane as shown in Figure 10. In both figures, the manipulator is actuated by one pulley attached with a velocity of approximately $1\,\frac{\text{mm}}{\text{s}}$. In Figure 10(a), movements are shown that result from the actuation of one tendon fixed in the

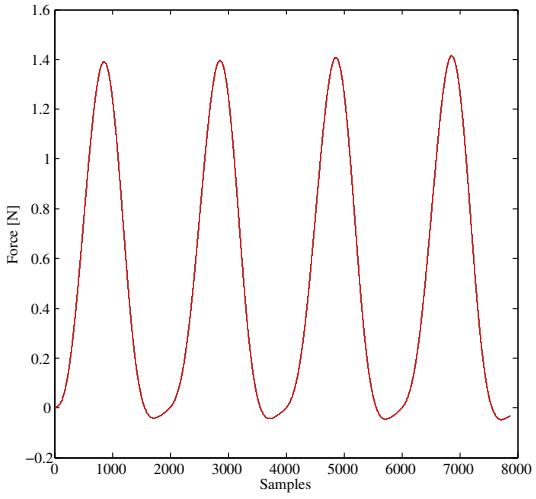

Fig. 6. Raw data of deflection tests at the manipulator tip with 0.015 MPa

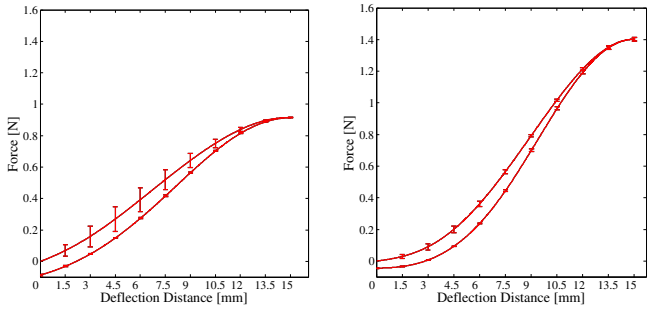

(a) (b)

Fig. 7. Deflection versus force at the manipulator tip ($\vec{F}_{x_1}$) for pressures of (a) 0.0075 MPa and (b) 0.015 MPa.

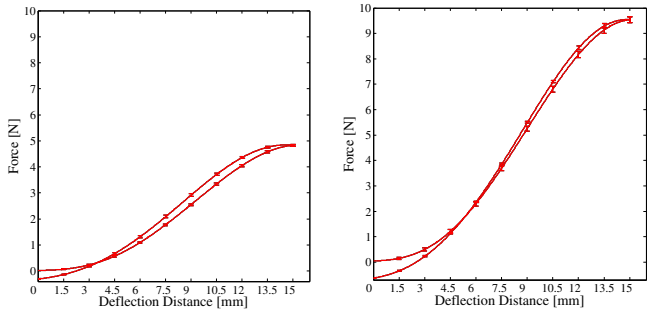

(a) (b)

Fig. 8. Deflection versus force at the center of the manipulator ($\vec{F}_{x_2}$) for pressures of (a) 0.0075 MPa and (b) 0.015 MPa.

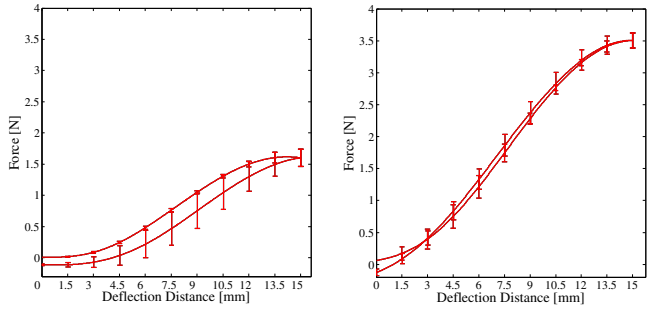

(a) (b)

Fig. 9. Deflection versus force at the tip of the manipulator ($\vec{F}_z$) for pressures of (a) 0.0075 MPa and (b) 0.015 MPa.

middle of the manipulator. In this case, only the bottom section bends (up to 90°); while the top section remains straight. Figure 10(b) shows the actuation of one tendon attached to the manipulator tip. The pulling force leads to a bending behavior of both sections at the same time changing the tip orientation by 180°. In both bending experiments, the internal pressure was set to 0.015 MPa and remained constant. Hence, an infinite range of bending configurations can be achieved combining simultaneous actuation of the three tendons and different level of internal pressure.

E. Squeezability in the Deflated State

As the manipulator is entirely soft and does not contain any solid material, it is able to achieve a high level of squeezability in terms of diameter and length between the inflated to deflated state. This behavior allows this novel manipulator to be squeezed through narrow openings. The overall size in the shrunk state is only limited by the thickness of the polyester fabric of the outer sleeve, the thickness of the latex bladder and the size of the tendons used. Figure 11 shows the squeezability of the robot. In Figure 11(a), the manipulator is inserted through an ENDOPATH XCEL Trocar of 18 mm diameter which is used in laparoscopic surgery. The trocar is placed through the abdominal wall of a phantom torso. Figure 11(b) shows the squeezed manipulator emerging on the other side of the Trocar inside the abdomen area. Though the robot is partially squeezed by the Trocar, its abilities to elongate and bend are still functional (Figures 11(b) and (c)).

V. DISCUSSION AND CONCLUSIONS

In this paper, a new hybrid actuation system for a robotic manipulator was explored combining pneumatic with tendon- driven actuation. This antagonistic actuation method took inspiration from biology. In fact, the octopus has longitudinal and transversal muscles in its arms. By activating both sets of muscles, the octopus arms can be stiffened. A similar behavior was achieved with the approach presented in this paper. It combines the advantages of tendon-driven and pneumatic actuated systems. The new approach goes beyond what state-of-the-art soft, flexible robots can achieve: Because the new robot is mainly made of thin fabric-like materials that are filled with air to achieve a fully-extended state, it can be shrunk to a considerably small size when entirely deflated. This capability to move between these two extreme states make the robot a particularly useful candidate for applications such as MIS as well as search and rescue.

A motion control system can be used to control the tendons and pressure at the same time. Keeping a constant pressure value, lateral and longitudinal deflections were applied to the manipulator. The recorded forces show a fairly proportional relationship with regards to the applied pressure. The hysteresis effects decreased in experiments where the robot's stiffness was high. Further, the robot was able to bend, to morph from entirely inflated to completely shrunk as well as to squeeze through narrow openings.

(a) (b)

Fig. 10. Single tendon actuation of the (a) bottom section and (b) top section.

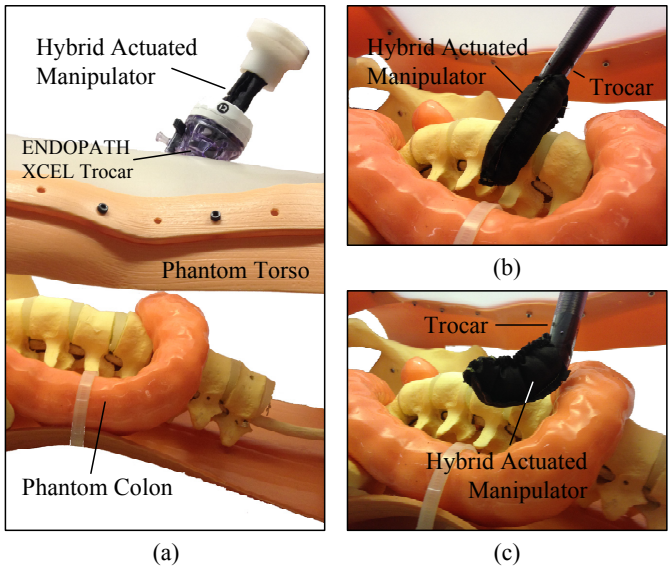

Fig. 11. The manipulator is squeezed through an ENDOPATH XCEL Trocar of 18 mm diameter.

In future work, we consider to enhance the fabrication of the hybrid actuation manipulator. When applying longitudinal forces or changing between the inflated and deflated state, the inner latex bladder tended to twist. Further research will also investigate to increase the stiffness of the manipulator and explore new designs which allow utilizing the empty space within the air-filled latex bladder, as possibly required when integrating sensors or actuators for additional tools such as tip-mounted grippers.

References

[1] G. Robinson and J. Davies, "Continuum robots - a state of the art," in *IEEE International Conference on Robotics and Automation*, 1999.

[2] I. D. Walker, "Robot strings: Long, thin continuum robots," in *IEEE Aerospace Conference*, 2013.

[3] A. Ataollahi, R. Karim, A. S. Fallah, K. Rhode, R. Razavi, L. Seneviratne, T. Schaeffter, and K. Althoefer, "3-dof mr-compatible multi-segment cardiac catheter steering mechanism," *IEEE Transactions on Biomedical Engineering*, vol. 99, 2013.

[4] I. Gravagne, C. Rahn, and I. D. Walker, "Large deflection dynamics and control for planar continuum robots," *IEEE/ASME Transactions on Mechatronics*, vol. 8, no. 2, pp. 299–307, 2003.

[5] D. Camarillo, C. Milne, C. Carlson, M. Zinn, and J. Salisbury, "Mechanics modeling of tendon-driven continuum manipulators," *IEEE Transactions on Robotics*, vol. 24, no. 6, pp. 1262–1273, 2008.

[6] R. Cieslak and A. Morecki, "Elephant trunk type elastic manipulator - a tool for bulk and liquid type materials transportation," *Robotica*, vol. 17, pp. 11–16, 1999.

[7] H. Watanabe, K. Kanou, Y. Kobayashi, and M. Fujie, "Development of a "steerable drill" for acl reconstruction to create the arbitrary trajectory of a bone tunnel," in *IEEE/RSJ International Conference on Intelligent Robots and Systems*, pp. 955–960, 2011.

[8] A. Deshpande, J. Ko, D. Fox, and Y. Matsuoka, "Control strategies for the index finger of a tendon-driven hand," *The International Journal of Robotics Research*, vol. 32, no. 1, pp. 115–128, 2013.

[9] M. Moses, M. Kutzer, H. Ma, and M. Armand, "A continuum manipulator made of interlocking fibers," in *IEEE International Conference on Robotics and Automation*, 2013.

[10] L. Kratchman, M. Rahman, J. Saunders, P. Swaney, and R. W. III, "Toward robotic needle steering in lung biopsy: a tendon-actuated approach," in *Medical Imaging: Visualization, Image-Guided Procedures, and Modeling*, 2011.

[11] S. Sanan, J. Moidel, and C. Atkeson, "A continuum approach to safe robots for physical human interaction," in *International Symposium on Quality of Life Technology*, 2011.

[12] L. Lyons, R. W. III, and R. Alterovitz, "Planning active cannula configurations through tubular anatomy," in *IEEE International Conference on Robotics and Automation*, pp. 2082–2087, 2010.

[13] C. Bedell, J. Lock, A. Gosline, and P. Dupont, "Design optimization of concentric tube robots based on task and anatomical constraints," in *IEEE International Conference on Robotics and Automation*, 2011.

[14] X. Lil, T. Choi, H. Chun, S. Gim, S. Lee, S. Kang, and K. Kim, "Active cannula robot with misorientation auto-recovery camera: A method to improve hand-eye coordination in minimally invasive surgery," in *International Conference on Control, Automation and Systems*, pp. 276–280, 2013.

[15] S. Neppalli, B. Jones, W. McMahan, V. Chitrakaran, I. Walker, M. Pritts, M. Csencsits, C. Rahn, and M. Grissom, "Octarm - a soft robotic manipulator," in *IEEE/RSJ International Conference on Intelligent Robots and Systems*, 2007.

[16] J. Shang, D. Noonan, C. Payne, J. Clark, M. Sodergren, A. Darzi, and G.-Z. Yang, "An articulated universal joint based flexible access robot for minimally invasive surgery," in *International Conference on Robotics and Automation*, pp. 1147–1152, 2011.

[17] M. Follador, M. Cianchetti, A. Arienti, and C. Laschi, "A general method for the design and fabrication of shape memory alloy active spring actuators," *Smart Materials And Structures*, vol. 21, 2012.

[18] A. Jiang, E. Secco, H. Wurdemann, T. Nanayakkara, P. Dasgupta, and K. Athoefer, "Stiffness-controllable octopus-like robot arm for minimally invasive surgery," in *3rd Joint Workshop on New Technologies for Computer/Robot Assisted Surgery*, 2013.

[19] Y. Noh, S. Sareh, J. Back, H. Wurdemann, T. Ranzani, E. Secco, A. Faragasso, H. Liu, and K. Althoefer, "A three-axial body force sensor for flexible manipulators," in *IEEE International Conference on Robotics and Automation*, 2014.

[20] S. Sareh, A. Jiang, A. Faragasso, Y. Noh, T. Nanayakkara, P. Dasgupta, L. Seneviratne, H. Wurdemann, and K. Althoefer, "Bio-inspired tactile sensor sleeve for surgical soft manipulators," in *IEEE International Conference on Robotics and Automation*, 2014.

[21] Y. Noh, E. Secco, S. Sareh, A. F. H.A. Wurdemann, J. Back, H. Liu, E. Sklar, and K. Althoefer, "A continuum body force sensor designed for flexible surgical robotic devices," in *IEEE Engineering in Medicine and Biology Society*, 2014.

[22] M. Cianchetti, T. Ranzani, G. Gerboni, I. de Falco, C. Laschi, and A. Menciassi, "Stiff-flop surgical manipulator: Mechanical design and experimental charaterization of the single module," in *IEEE/RSJ International Conference on Intelligent Robots and Systems*, 2013.

[23] A. Jiang, T. Aste, P. Dasgupta, K. Althoefer, and T. Nanayakkara, "Granular jamming with hydraulc control," in *ASME International Design Engineering Technical Conferences & Computers and Information in Engineering Conference*, 2013.

[24] D. Caldwell, G. Medrano-Cerda, and M. Goodwin, "Control of pneumatic muscle actuators," *IEEE Control Systems*, vol. 15, 1995.

[25] A. Jiang, G. Xynogalas, P. Dasgupta, K. Althoefer, and T. Nanayakkara, "Design of a variable stiffness flexible manipulator with composite granular jamming and membrane coupling," in *IEEE/RSJ International Conference on Intelligent Robots and Systems*, 2012.

[26] D. Shin, I. Sardellitti, and O. Khatib, "A hybrid actuation approach for human-friendly robot design," in *IEEE International Conference on Robotics and Automation*, pp. 1747–1752, 2008.

[27] G. Immega and K. Antonelli, "The KSI tentacle manipulator," in *IEEE International Conference on Robotics and Automation*, 1995.

[28] B. Jones, W. McMahan, and I. Walker, "Design and analysis of a novel pneumatic manipulator," in *IFAC Symposium "Advances in Automotive Control"*, 2004.

[29] Y. Gutfreund, T. Flash, G. Fiorito, and B. Hochner, "Patterns of arm muscle activation involved in octopus reaching movements," *The Journal of Neuroscience*, vol. 18, no. 15, p. 5976598, 1998.

[30] C. Laschi, B. Mazzolai, V. Mattoli, M. Cianchetti, and P. Dario, "Design of a biomimetic robotic octopus arm," *Bioinspiration and Biomimetics*, vol. 4, pp. 1–8, 2009.

[31] M. Cianchetti, A. Arienti, M. Follador, B. Mazzolai, P. Dario, and C. Laschi, "Design concept and validation of a robotic arm inspired by the octopus," *Materials Science and Engineering C*, vol. 31, p. 12301239, 2011.